Table VI. Bond Length Comparisons Showing the Effect of Buttressing Ligands[a]

metal	M–M bond dist, Å				diff
	buttressed		unbuttressed		
Nb	$Nb_2Cl_6(dmpm)_2$	2.711 (3)	$Nb_2Cl_6(dppe)_2$	2.729 (2)	~0
			$Nb_2Cl_6(dppm)_2$	2.696 (1)	
Ta	$TaCl_6(dmpm)_2$	2.692 (2)	$Ta_2Cl_6(PMe_3)_4$	2.721 (1)	~0.02
			$Ta_2Cl_6(dmpe)_2$	2.710 (1)	
Mo	$Mo_2Cl_6(dppm)_2$	2.789 (1)	$Mo_2Cl_6(depe)_2$	2.785 (3)[b]	~0
			$Mo_2Cl_6(dppe)_2$	2.762 (1)[b]	
W	$W_2Cl_6(dppm)_2$	2.691 (1)[c]	$W_2Cl_6(PMe_3)_4$	2.711 (1)[d]	0.02
Re	$Re_2Cl_6(dppm)_2$	2.667 (1)	$Re_2Cl_6(dppe)_2$	3.809 (1)	1.14
Ru	$Ru_2Cl_6(dmpm)_2$	2.933 (1)[e]	$Ru_2Cl_6(PBu_3)_4$	3.733 (2)[f]	0.80

[a] Unreferenced data are found in ref 1. A few other compounds might have been included but would not change the picture. [b] Reference 4. [c] Reference 3. [d] Chisholm, M. H. private communication. [e] This compound is listed in the table in ref 1 but mistakenly shown as $Ru_2Cl_6(dppm)_2$. [f] Cotton, F. A.; Matusz, M.; Torralba, R. C. *Inorg. Chem.* **1989**, *28*, 1516.

ligand in each (dmpm), there is an increase of 0.35 Å, attributable to the loss of the π component of M–M bonding. We cannot directly compare Ru and Rh compounds with the same ligand, but it is probably safe to do so indirectly by noting that, for Mo, W, and Re, the change from dmpm to dppm ligands causes an increase of ca. 0.04 Å in the M–M distances. We might thus estimate that, for the $Ru_2Cl_6(dppm)_2$ molecule, the Ru–Ru distance would be 2.93 + 0.04 = 2.97 Å. Thus, on loss of the σ bond as we go from $Ru_2Cl_6(dppm)_2$ to $Rh_2Cl_6(dppm)_2$, the increase is ca. 0.45 Å. This greater increase presumably reflects the greater strength of the σ bond compared to the π bond.

Comparison of the Rh–Rh distances in $Rh_2Cl_6(dppm)_2$ and $Rh_2Br_6(dppm)_2$ shows that the expected effect of increasing the size of the bridging atoms translates into an approximately 0.10-Å increase in the metal–metal distance for this type of compound. Whether this number will be, approximately, valid more generally remains to be seen. No other such direct comparison seems yet to have been reported.[1]

Finally, the increase in Rh–Rh distance from the buttressed case of $Rh_2Cl_6(dppm)_2$ to the unbuttressed case of $Rh_2Cl_6(PBu_3)_4$ of about 0.3 Å invites comparison with similar pairs of compounds formed by M(III) metal atoms where, unlike the Rh case, M–M bonding occurs—or can occur. Pertinent data are gathered in Table VI. Clearly, in cases where there are d^2 and d^3 M(III) atoms, which form bonds of order 2, the buttressing effect is not seen. Presumably in these cases the drive to form M–M bonds is so strong, and the bonds formed are intrinsically so short (2.68–2.78 Å), that the buttressing ligands, dmpm and dppm, do little to affect them. When we reach the d^4–d^4 case, as exemplified by Re(III), there is clearly an enormous change. Here, in the absence of the buttressing type of ligand no M–M bond formation occurs at all (Re···Re = 3.81 Å), while the use of a buttressing ligand leads to M–M bond formation and indeed to the formation of a very strong, short (2.67 Å) bond of order 2.

It is *not* evident why this discontinuous change in behavior occurs, but it *is* evident that the pattern persists as we go to the d^5–d^5 case as exemplified by Ru(III). Here again, in the absence of the buttressing effect, there is no M–M bond (Ru···Ru = 3.73 Å) whereas when two of the dmpm buttressing ligands are present, a net single bond (2.93 Å) is formed.

In the case of d^6–d^6 exemplified by Rh(III), there is no M–M bond formed under any circumstances, as expected. The 0.3-Å shortening caused by the use of buttressing ligands shows that a "buttressing effect", when not covered up or overwhelmed by any other effect (e.g., M–M bonding), can be appreciable when the M···M distances are large (ca. 3.5 Å) but still not nearly capable of drawing the M atoms as close together as they are drawn by even a single bond (i.e., <3.0 Å in the Ru(III) case).

Acknowledgment. We are grateful to the National Science Foundation for support, and we thank F. L. Campbell, III, for assistance.

Supplementary Material Available: For both crystal structures, full tables of crystal parameters and details of data collection and refinement, bond distances, bond angles, and anisotropic displacement parameters and, for $Rh_2Cl_6(dppm)_2 \cdot 3C_6H_6 \cdot 2CH_2Cl_2$, a table of H atom coordinates with isotropic displacement parameters and a detailed account of how the interstitial solvent molecules were refined (15 pages); tables of observed and calculated structure factors (36 pages). Ordering information is given on any current masthead page.

Contribution from the Institut für Physikalische
und Theoretische Chemie and Physikalisches Institut,
Abt. II, University of Erlangen-Nürnberg,
D-8520 Erlangen, West Germany, and Laboratoire de
Spectrochimie des Eléments de Transition,
Université de Paris-Sud, F-91405 Orsay, France

X-ray Powder Diffraction at the Spin-State Transition in [*N*,*N'*-Ethylenebis(3-carboxysalicylaldiminato)]cobalt(II) Complexes

E. König,*[1a] G. Ritter,[1b] J. Dengler,[1b] P. Thuéry,[2] and J. Zarembowitch*[2]

Received June 29, 1988

Although thermally induced spin-state transitions may arise for compounds of transition metals with electronic configurations d^4, d^5, d^6, d^7, and d^8, most experimental studies have been confined to those of iron(II), iron(III), and cobalt(II).[3-5] Two different types of transition may be readily distinguished: (i) discontinuous transitions, which are characterized by an abrupt change of the relevant physical properties, thus defining the transition temperature, T_c; (ii) continuous transitions, which show a gradual variation of the physical properties over an extended range of temperature (T_c being defined by the temperature where the high-spin fraction $n_{HS} = 0.50$).[4] Spin-state transitions are accompanied by a significant modification of molecular geometry, the most remarkable being the variation in the metal–donor atom distance.[6] The coordination sphere volume becomes smaller on passing from the high-spin (HS) to the low-spin (LS) state, which generally results in a lowering of the molecular volume.

For a number of iron(II) spin transition systems, it has been shown[4] that a clear distinction between the two types of transition may be achieved by the study of X-ray powder diffraction over a range of temperatures inclusive of T_c. For discontinuous transitions, distinct and individual X-ray diffraction patterns for the two spin states, HS and LS, are observed. In the transition region, these patterns replace each other as the transition progresses in either direction, one diminishing while the other gains in intensity. The temperature dependence of the relative intensity I_{HS}/I_{tot} conforms to the temperature variation of n_{HS} as determined from, for example, the temperature dependence of magnetism. For continuous transitions a single X-ray diffraction pattern is in general encountered, the Bragg angle for any particular line displaying a continuous shift in the transition region. This shift is a consequence of the variation in unit cell volume and the associated change of lattice parameters in the course of the LS $\rightleftharpoons$ HS transition and thus exceeds by far the normal temperature shift of the reflections.

It is of interest to determine whether results analogous to those for iron(II) complexes can be established for spin-state transitions of other transition-metal ions. In this paper, we report, therefore, the first study of high-resolution X-ray powder diffraction in the spin-transition region for cobalt(II) complexes. The two six-coordinate compounds chosen are $Co(H_2fsa_2en)(py)_2$ (A) and Co-

---

(1) (a) Institut für Physikalische und Theoretische Chemie, University of Erlangen-Nürnberg. (b) Physikalisches Institut, Abt. II, University of Erlangen-Nürnberg.

(2) Laboratoire de Spectrochimie des Eléments de Transition, Université de Paris-Sud.

(3) Gütlich, P. *Struct. Bonding* **1981**, *44*, 83.

(4) König, E.; Ritter, G.; Kulshreshtha, S. K. *Chem. Rev.* **1985**, *85*, 219.

(5) Martin, R. L.; White, A. H. *Transition Met. Chem.* (*N.Y.*) **1968**, *4*, 113.

(6) König, E. *Prog. Inorg. Chem.* **1987**, *35*, 527.

0020-1669/89/1328-1757$01.50/0

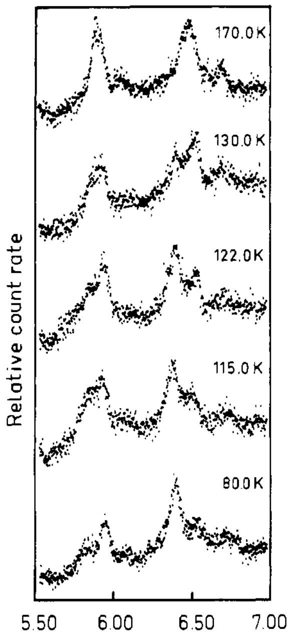

Figure 1. X-ray powder diffraction peak profiles for $Co(H_2fsa_2en)(py)_2$ over the temperature interval 170.0–80.0 K for Bragg angles between 5.50 and 7.00°. The measurements have been performed for increasing temperatures.

$(H_2fsa_2en)(4\text{-}t\text{-}Bupy)_2$ (B), where $H_2fsa_2en^{2-}$ is the phenolic dianion of the Schiff base *N*,*N'*-ethylenebis(3-carboxysalicylaldimine), py denotes pyridine, and *t*-Bu a *tert*-butyl substituent. Both compounds exhibit a discontinuous type spin-state transition between the $S = {}^3/_2$ and $S = {}^1/_2$ ground states of cobalt(II), the transition temperatures having been reported[7,8] as $T_c^{\downarrow} = 115$ K, $T_c^{\uparrow} = 127$ K for A and $T_c^{\downarrow} = 138$ K, $T_c^{\uparrow} = 154$ K for B for decreasing and increasing temperature, respectively. These transitions are among the most abrupt ever observed for cobalt(II) complexes, both being associated with a hysteresis of widths $\Delta T_c = 12$ K for A and $\Delta T_c = 16$ K for B.

Experimental Section

Materials. Compounds A and B were prepared by the methods previously described.[7,8] The purity of the substances was checked by elemental analysis and magnetic measurements.

Measurements. X-ray powder diffraction was measured with a Siemens counter diffractometer using Cu Kα radiation. Variable temperatures were obtained with an Oxford Instruments CF108A continuous-flow cryostat and liquid nitrogen as coolant. Temperatures were measured by a calibrated resistance thermometer, temperature stability of ±0.1 K being achieved. The angular steps of the diffractometer were 0.02 and 0.005° in terms of 2θ. The resulting pulses were stored in an Elscint MEDA 10 multichannel analyzer, and the data were processed on an Olivetti M28 PC and fitted to Gaussian line shape.

Magnetic susceptibilities were measured with a Faraday type magnetometer equipped with an Oxford Instruments continuous-flow cryostat. The set temperature was maintained to within about ±0.1 K. $HgCo(SCN)_4$ was used as the susceptibility standard, and the data were corrected for diamagnetism.[7,8] Values of n_{HS} were determined from the measured molar susceptibility values χ_M according to $n_{HS} = [\chi_M T - (\chi_M T)_{LS}]/[(\chi_M T)_{HS} - (\chi_M T)_{LS}]$. The values for the pure HS and LS states of $Co(H_2fsa_2en)(py)_2$ were taken as $(\chi_M T)_{HS} = 2.70$ cm^3 mol^{-1} K (the room-temperature value obtained for the sample under study) and $(\chi_M T)_{LS} = 0.46$ cm^3 mol^{-1} K.[7]

Results

In Figure 1 the X-ray diffraction peak profiles for $Co(H_2fsa_2en)(py)_2$ measured for the Bragg angle range 5.50–7.00° are displayed for increasing temperatures. The corresponding results for the angle range 11.75–12.75° are shown in Figure 2. The data are plotted over the temperature intervals 170.0–80.0 and 170.0–115.0 K, respectively. The results for decreasing temperatures, which are not shown in detail, are similar except for a shift in temperature. Magnetic susceptibilities were obtained for the actual sample used for X-ray powder diffraction measurements, the results being shown in Figure 3 in terms of n_{HS}. Included in Figure 3 is the relative intensity I_{HS}/I_{tot} of the X-ray diffraction peak at 12.30°.

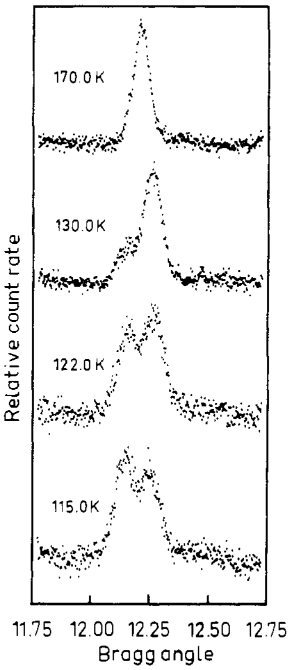

Figure 2. X-ray powder diffraction peak profiles for $Co(H_2fsa_2en)(py)_2$ over the temperature interval 170.0–115.0 K for Bragg angles between 11.75 and 12.75°. The measurements have been performed for increasing temperatures.

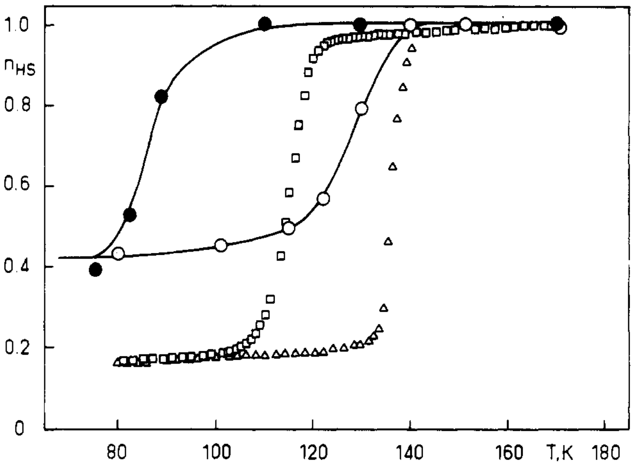

Figure 3. Temperature dependence of the HS fraction n_{HS} from magnetic susceptibility measurements for $Co(H_2fsa_2en)(py)_2$: ▲, increasing temperature; □, decreasing temperature ($T_c^{\uparrow} = 136$ K; $T_c^{\downarrow} = 114$ K). Included are values of the relative intensity of X-ray diffraction I_{HS}/I_{tot} based on the peak at 12.30°: ○, increasing temperature; ●, decreasing temperature.

The overall X-ray powder diffraction pattern for the complex $Co(H_2fsa_2en)(4\text{-}t\text{-}Bupy)_2$ is presented in Figure 4 for the temperature interval 230.0–80.0 K. The measurements for Bragg angles between 3.0 and 12.0° have been obtained for decreasing temperature.

Discussion

For $Co(H_2fsa_2en)(py)_2$, initial X-ray powder diffraction has been measured for temperatures between 248.0 and 80.0 K over the complete range of Bragg angles between 3.0 and 13.0°, for both increasing and decreasing temperature. The peak profiles for increasing temperatures presented in Figures 1 and 2 show

---

(7) Zarembowitch, J.; Kahn, O. *Inorg. Chem.* **1984**, *23*, 589.

(8) Thuéry, P.; Zarembowitch, J. *Inorg. Chem.* **1986**, *25*, 2001.

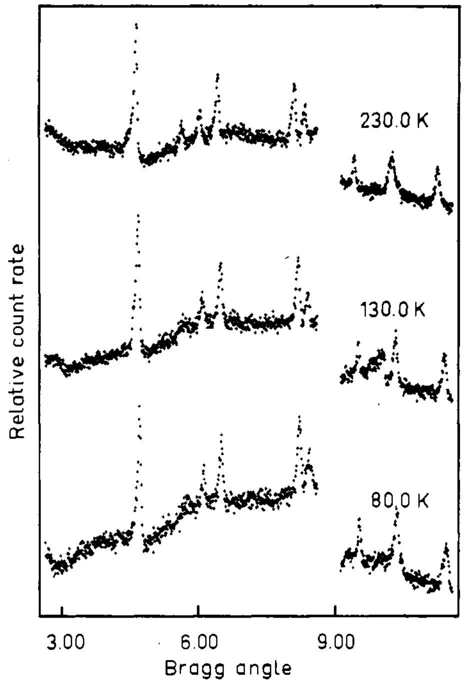

Figure 4. X-ray powder diffraction for Co(H_2fsa$_2$en)(4-*t*-Bupy)$_2$ over the temperature interval 230.0–80.0 K for decreasing temperatures.

regions in the diffraction angle range where the observed changes are particularly marked. It is clearly seen that, in the transition region, the individual patterns for the HS and LS states replace each other as the transition progresses. This observation is in agreement with the first-order character of the transition[7] and conforms to the general behavior of discontinuous spin-state transitions in compounds of iron(II).[4] According to Figure 3, the transition temperatures for the actual sample as determined on the basis of magnetic measurements are $T_c^{\downarrow} = 114$ K and $T_c^{\uparrow} = 136$ K. The value of $T_c^{\uparrow}$ is somewhat different from that published earlier,[7] which is not surprising since spin-state characteristics are known to be generally dependent on the solid-state properties of the sample.[4] A much larger discrepancy is shown by the hysteresis derived from I_{HS}/I_{tot} values of the X-ray diffraction data, which lead to the apparent transition temperatures $T_c^{\downarrow} \simeq 85$ K and $T_c^{\uparrow} \simeq 126$ K. This discrepancy is certainly too large to be attributed to differences of calibration of the temperature readings. It should be noted that the I_{HS}/I_{tot} values employed in the figure are based on the peak at 12.30°; cf. Figure 2. Most other major diffraction peaks show too much overlap with neighboring lines such that even a decomposition into Gaussians does not provide reliable values for the intensity of an individual line. This fact could introduce some uncertainty of I_{HS}/I_{tot} values, although a larger shift of the transition temperature is difficult to visualize. In particular, inspection of Figures 1 and 2 clearly demonstrates that the most conspicuous change of diffraction pattern occurs between 122.0 and 130.0 K. The difference between the hysteresis loop derived from X-ray diffraction and that obtained on the basis of magnetic data rather resembles the hysteresis differences found for some other spin-transition compounds, such as [Fe(4,7-(CH_3)$_2$-phen)$_2$(NCS)$_2$]·$^1/_2$(α-picoline)[9] and [Fe(3-OCH_3-SalEen)$_2$]PF_6,[10] as the result of intensive grinding of the sample. Although the compounds in the present study were used as obtained, cycling of temperature could break the crystallites into smaller fragments. The effect expected for this situation[9] is similar to that of grinding[9,10] or the application of pressure,[7,11] i.e. a more gradual appearance of the transition, increased n_{HS} values at low temperatures due to a more incomplete transformation of spin state, and a lowering of the temperature where $n_{HS} = 0.50$, i.e. of the apparent transition temperatures $T_c^{\uparrow}$ and $T_c^{\downarrow}$. This is indeed what is observed for the results of Figure 3.

A single-crystal X-ray diffraction study of Co(H_2fsa$_2$en)(py)$_2$ in the HS state has been recently carried out.[12] According to this study, the cobalt(II) ion is in a distorted octahedral environment with an apical metal–donor atom bond length of 2.262 Å and a mean equatorial bond length of 2.079 Å. The comparison of structural data for various square-pyramidal HS and LS cobalt(II) compounds indicates[13] an overall bond length change of 0.09 Å. This is significantly smaller than the change normally accompanying a spin change in iron(II) (~0.18 Å).[6] The average change for equatorial Co–N bonds has been found as ≃0.15 – 0.21 Å, and that for equatorial Co–O bonds, as 0.04–0.07 Å. Recent EXAFS measurements performed at 295 and 40 K arrived at average bond length changes of 0.09 and 0.12 Å for the spin-state transitions in Co(H_2fsa$_2$en)(H_2O)$_2$ and Co(H_2fsa$_2$en)(py)$_2$, respectively.[13] It should be noted that the $\Delta S = 1$ spin-state change in cobalt(II) involves only a single electron ($t_{2g}^6e_g^1 \leftrightarrow t_{2g}^5e_g^2$). Consequently, the metal–ligand bond length variation and the observable change of powder diffraction are expected to be generally smaller than for complexes of iron(II) or iron(III).

For Co(H_2fsa$_2$en)(4-*t*-Bupy)$_2$, the X-ray powder diffraction has been measured for a number of temperatures between 230.0 and 80.0 K. As is evident from Figure 4, no major change of the resulting pattern due to the variation of temperature is apparent, not even in the transition region. It has been verified on the basis of magnetic susceptibility measurements performed on the same sample that the transition takes place at $T_c^{\downarrow} = 136.5$ K for decreasing and at $T_c^{\uparrow} = 150$ K for increasing temperature. The values of the transition temperature show a slight difference from the values published previously.[8] The absence of any observable change in the X-ray powder diffraction for this compound on spin-state transition is surprising. However, it should be noted that many individual reflections of the crystallites may at least partly overlap, and thus the variation expected for HS and LS states could easily be concealed under the relatively broad powder peaks.

Acknowledgment. The authors appreciate financial support from the Deutsche Forschungsgemeinschaft, Bonn, West Germany. Critical reading of the manuscript by H. A. Goodwin, Sydney, is gratefully acknowledged.

Registry No. Co(H_2fsa$_2$en)(py)$_2$, 70995-74-3; Co(H_2fsa$_2$en)(4-*t*-Bupy)$_2$, 102109-99-9.

---

(9) König, E.; Ritter, G.; Kulshreshtha, S. K.; Csatary, N. *Inorg. Chem.* **1984**, *23*, 1903.
(10) Haddad, M. S.; Federer, W. D.; Lynch, M. W.; Hendrickson, D. N. *Inorg. Chem.* **1981**, *20*, 131.
(11) König, E.; Ritter, G.; Waigel, J.; Goodwin, H. A. *J. Chem. Phys.* **1985**, *83*, 3055.
(12) Charpin, P.; Nierlich, M.; Vigner, D.; Lance, M.; Thuéry, P.; Zarembowitch, J.; d'Yvoire, F. *J. Crystallogr. Spectrosc. Res.* **1988**, *18*, 429.1.
(13) Thuéry, P.; Zarembowitch, J.; Michalowicz, A.; Kahn, O. *Inorg. Chem.* **1987**, *26*, 851.

Contribution from the Department of Chemistry,
Metcalf Center for Science and Engineering,
Boston University, Boston, Massachusetts 02215

Applications of the Quantitative Analysis of Ligand Effects (QALE). Steric Profiles for Reactions Involving "Spectator" Phosphorus(III) Ligands

Klaas Eriks,* Warren P. Giering,* Hong-Ye Liu,
and Alfred Prock*

Received November 23, 1988

"Spectator" phosphorus(III) ligands of organometallic complexes do not directly participate in chemistry at a metal center. Since spectator ligands remain in the coordination sphere of the metal, they influence the energies of the ground- and transition-state energies through transmission of their stereo–electronic properties to the metal center. Transition-metal reactions where